The Astrophysical Journal, 938:38 (11pp), 2022 October 10 https://doi.org/10.3847/1538-4357/ac8de4

Search for Astrophysical Neutrinos from 1FLE Blazars with IceCube

R. Abbasi[1], M. Ackermann[2], J. Adams[3], J. A. Aguilar[4], M. Ahlers[5], M. Ahrens[6], J. M. Alameddine[7], A. A. Alves, Jr.[8], N. M. Amin[9], K. Andeen[10], T. Anderson[11], G. Anton[12], C. Argüelles[13], Y. Ashida[14], S. Athanasiadou[2], S. Axani[15], X. Bai[16], A. Balagopal V.[14], M. Baricevic[14], S. W. Barwick[17], V. Basu[14], R. Bay[18], J. J. Beatty[19,20], K.-H. Becker[21], J. Becker Tjus[22], J. Beise[23], C. Bellenghi[24], S. Benda[14], S. BenZvi[25], D. Berley[26], E. Bernardini[2,62], D. Z. Besson[27], G. Binder[18,28], D. Bindig[21], E. Blaufuss[26], S. Blot[2], F. Bontempo[8], J. Y. Book[13], J. Borowka[29], S. Böser[30], O. Botner[23], J. Böttcher[29], E. Bourbeau[5], F. Bradascio[2], J. Braun[14], B. Brinson[31], S. Bron[32], J. Brostean-Kaiser[2], R. T. Burley[33], R. S. Busse[34], M. A. Campana[35], E. G. Carnie-Bronca[33], C. Chen[31], Z. Chen[36], D. Chirkin[14], K. Choi[37], B. A. Clark[38], L. Classen[34], A. Coleman[9], G. H. Collin[15], A. Connolly[19,20], J. M. Conrad[15], P. Coppin[39], P. Correa[39], D. F. Cowen[11,40], R. Cross[25], C. Dappen[29], P. Dave[31], C. De Clercq[39], J. J. DeLaunay[41], D. Delgado López[13], H. Dembinski[9], K. Deoskar[6], A. Desai[14], P. Desiati[14], K. D. de Vries[39], G. de Wasseige[42], T. DeYoung[38], A. Diaz[15], J. C. Díaz-Vélez[14], M. Dittmer[34], H. Dujmovic[8], M. A. DuVernois[14], T. Ehrhardt[30], P. Eller[24], R. Engel[8,43], H. Erpenbeck[29], J. Evans[26], P. A. Evenson[9], K. L. Fan[26], A. R. Fazely[44], A. Fedynitch[45], N. Feigl[46], S. Fiedlschuster[12], A. T. Fienberg[11], C. Finley[6], L. Fischer[2], D. Fox[40], A. Franckowiak[2,22], E. Friedman[26], A. Fritz[30], P. Fürst[29], T. K. Gaisser[9], J. Gallagher[47], E. Ganster[29], A. Garcia[13], S. Garrappa[2], L. Gerhardt[28], A. Ghadimi[41], C. Glaser[23], T. Glauch[24], T. Glüsenkamp[12], N. Goehlke[43], J. G. Gonzalez[9], S. Goswami[41], D. Grant[38], T. Grégoire[11], S. Griswold[25], C. Günther[29], P. Gutjahr[7], C. Haack[24], A. Hallgren[23], R. Halliday[38], L. Halve[29], F. Halzen[14], H. Hamdaoui[36], M. Ha Minh[24], K. Hanson[14], J. Hardin[14,15], A. A. Harnisch[38], P. Hatch[48], A. Haungs[8], K. Helbing[21], J. Hellrung[29], F. Henningsen[24], E. C. Hettinger[38], L. Heuermann[29], S. Hickford[21], J. Hignight[49], C. Hill[50], G. C. Hill[33], K. D. Hoffman[26], K. Hoshina[14,63], W. Hou[8], M. Huber[24], T. Huber[8], K. Hultqvist[6], M. Hünnefeld[7], R. Hussain[14], K. Hymon[7], S. In[37], N. Iovine[4], A. Ishihara[50], M. Jansson[6], G. S. Japaridze[51], M. Jeong[37], M. Jin[13], B. J. P. Jones[52], D. Kang[8], W. Kang[37], X. Kang[35], A. Kappes[34], D. Kappesser[30], L. Kardum[7], T. Karg[2], M. Karl[24], A. Karle[14], U. Katz[12], M. Kauer[14], J. L. Kelley[14], A. Kheirandish[11], K. Kin[50], J. Kiryluk[36], S. R. Klein[18,28], A. Kochocki[38], R. Koirala[9], H. Kolanoski[46], T. Kontrimas[24], L. Köpke[30], C. Kopper[38], S. Kopper[41], D. J. Koskinen[5], P. Koundal[8], M. Kovacevich[35], M. Kowalski[2,46], T. Kozynets[5], E. Krupczak[38], E. Kun[22], N. Kurahashi[35], N. Lad[2], C. Lagunas Gualda[2], M. J. Larson[26], F. Lauber[21], J. P. Lazar[13,14], J. W. Lee[37], K. Leonard[14], A. Leszczyńska[9], M. Lincetto[22], Q. R. Liu[14], M. Liubarska[49], E. Lohfink[30], C. J. Lozano Mariscal[34], L. Lu[14], F. Lucarelli[32], A. Ludwig[38,53], W. Luszczak[14], Y. Lyu[18,28], W. Y. Ma[2], J. Madsen[14], K. B. M. Mahn[38], Y. Makino[14], S. Mancina[14], W. Marie Sainte[14], I. C. Mariş[4], I. Martinez-Soler[13], R. Maruyama[54], S. McCarthy[14], T. McElroy[49], F. McNally[55], J. V. Mead[5], K. Meagher[14], S. Mechbal[2], A. Medina[20], M. Meier[50], S. Meighen-Berger[24], Y. Merckx[39], J. Micallef[38], D. Mockler[4], T. Montaruli[32], R. W. Moore[49], R. Morse[14], M. Moulai[14], T. Mukherjee[8], R. Naab[2], R. Nagai[50], U. Naumann[21], J. Necker[2], L. V. Nguyễn[38], H. Niederhausen[38], M. U. Nisa[38], S. C. Nowicki[38], A. Obertacke Pollmann[21], M. Oehler[8], B. Oeyen[56], A. Olivas[26], J. Osborn[14], E. O'Sullivan[23], H. Pandya[9], D. V. Pankova[11], N. Park[48], G. K. Parker[52], E. N. Paudel[9], L. Paul[10], C. Pérez de los Heros[23], L. Peters[29], J. Peterson[14], S. Philippen[29], S. Pieper[21], A. Pizzuto[14], M. Plum[16], Y. Popovych[30], A. Porcelli[56], M. Prado Rodriguez[14], B. Pries[38], G. T. Przybylski[28], C. Raab[4], J. Rack-Helleis[30], A. Raissi[3], M. Rameez[5], K. Rawlins[57], I. C. Rea[24], Z. Rechav[14], A. Rehman[9], P. Reichherzer[22], G. Renzi[4], E. Resconi[24], S. Reusch[2], W. Rhode[7], M. Richman[35], B. Riedel[14], E. J. Roberts[33], S. Robertson[18,28], S. Rodan[37], G. Roellinghoff[37], M. Rongen[30], C. Rott[37,58], T. Ruhe[7], D. Ryckbosch[56], D. Rysewyk Cantu[38], I. Safa[13,14], J. Saffer[43], D. Salazar-Gallegos[38], P. Sampathkumar[8], S. E. Sanchez Herrera[38], A. Sandrock[7], M. Santander[41], S. Sarkar[49], S. Sarkar[59], K. Satalecka[2], M. Schaufel[29], H. Schieler[8], S. Schindler[12], T. Schmidt[26], A. Schneider[14], J. Schneider[12], F. G. Schröder[8,9], L. Schumacher[24], G. Schwefer[29], S. Sclafani[35], D. Seckel[9], S. Seunarine[60], A. Sharma[23], S. Shefali[43], N. Shimizu[50], M. Silva[14], B. Skrzypek[13], B. Smithers[52], R. Snihur[14], J. Soedingrekso[7], A. Sogaard[5], D. Soldin[9], C. Spannfellner[24], G. M. Spiczak[60], C. Spiering[2], M. Stamatikos[20], T. Stanev[9], R. Stein[2], J. Stettner[29], T. Stezelberger[28], T. Stürwald[21], T. Stuttard[5], G. W. Sullivan[26], I. Taboada[31], S. Ter-Antonyan[44], W. G. Thompson[13], J. Thwaites[14], S. Tilav[9], K. Tollefson[38], C. Tönnis[61], S. Toscano[4], D. Tosi[14], A. Trettin[2], M. Tselengidou[12], C. F. Tung[31], A. Turcati[24], R. Turcotte[8], J. P. Twagirayezu[38], B. Ty[14], M. A. Unland Elorrieta[34], M. Unland Elorrieta[34], K. Upshaw[44], N. Valtonen-Mattila[23], J. Vandenbroucke[14], N. van Eijndhoven[39], D. Vannerom[15], J. van Santen[2], J. Veitch-Michaelis[14], S. Verpoest[56], C. Walck[6], W. Wang[14], T. B. Watson[52], C. Weaver[38], P. Weigel[15], A. Weindl[8], J. Weldert[30], C. Wendt[14], J. Werthebach[7], M. Weyrauch[8], N. Whitehorn[38,53], C. H. Wiebusch[29], N. Willey[38], D. R. Williams[41], M. Wolf[14], G. Wrede[12], J. Wulff[22], X. W. Xu[44], J. P. Yanez[49], E. Yildizci[14], S. Yoshida[50], S. Yu[38], T. Yuan[14], Z. Zhang[36], and P. Zhelnin[13]

IceCube Collaboration

[1] Department of Physics, Loyola University Chicago, Chicago, IL 60660, USA; analysis@icecube.wisc.edu
[2] DESY, D-15738 Zeuthen, Germany
[3] Dept. of Physics and Astronomy, University of Canterbury, Private Bag 4800, Christchurch, New Zealand

[4] Université Libre de Bruxelles, Science Faculty CP230, B-1050 Brussels, Belgium
[5] Niels Bohr Institute, University of Copenhagen, DK-2100 Copenhagen, Denmark
[6] Oskar Klein Centre and Dept. of Physics, Stockholm University, SE-10691 Stockholm, Sweden
[7] Dept. of Physics, TU Dortmund University, D-44221 Dortmund, Germany
[8] Karlsruhe Institute of Technology, Institute for Astroparticle Physics, D-76021 Karlsruhe, Germany
[9] Bartol Research Institute and Dept. of Physics and Astronomy, University of Delaware, Newark, DE 19716, USA
[10] Department of Physics, Marquette University, Milwaukee, WI, 53201, USA
[11] Dept. of Physics, Pennsylvania State University, University Park, PA 16802, USA
[12] Erlangen Centre for Astroparticle Physics, Friedrich-Alexander-Universität Erlangen-Nürnberg, D-91058 Erlangen, Germany
[13] Department of Physics and Laboratory for Particle Physics and Cosmology, Harvard University, Cambridge, MA 02138, USA
[14] Dept. of Physics and Wisconsin IceCube Particle Astrophysics Center, University of Wisconsin–Madison, Madison, WI 53706, USA
[15] Dept. of Physics, Massachusetts Institute of Technology, Cambridge, MA 02139, USA
[16] Physics Department, South Dakota School of Mines and Technology, Rapid City, SD 57701, USA
[17] Dept. of Physics and Astronomy, University of California, Irvine, CA 92697, USA
[18] Dept. of Physics, University of California, Berkeley, CA 94720, USA
[19] Dept. of Astronomy, Ohio State University, Columbus, OH 43210, USA
[20] Dept. of Physics and Center for Cosmology and Astro-Particle Physics, Ohio State University, Columbus, OH 43210, USA
[21] Dept. of Physics, University of Wuppertal, D-42119 Wuppertal, Germany
[22] Fakultät für Physik & Astronomie, Ruhr-Universität Bochum, D-44780 Bochum, Germany
[23] Dept. of Physics and Astronomy, Uppsala University, Box 516, SE-75120 Uppsala, Sweden
[24] Physik-department, Technische Universität München, D-85748 Garching, Germany
[25] Dept. of Physics and Astronomy, University of Rochester, Rochester, NY 14627, USA
[26] Dept. of Physics, University of Maryland, College Park, MD 20742, USA
[27] Dept. of Physics and Astronomy, University of Kansas, Lawrence, KS 66045, USA
[28] Lawrence Berkeley National Laboratory, Berkeley, CA 94720, USA
[29] III. Physikalisches Institut, RWTH Aachen University, D-52056 Aachen, Germany
[30] Institute of Physics, University of Mainz, Staudinger Weg 7, D-55099 Mainz, Germany
[31] School of Physics and Center for Relativistic Astrophysics, Georgia Institute of Technology, Atlanta, GA 30332, USA
[32] Département de physique nucléaire et corpusculaire, Université de Genève, CH-1211 Genève, Switzerland
[33] Department of Physics, University of Adelaide, Adelaide, 5005, Australia
[34] Institut für Kernphysik, Westfälische Wilhelms-Universität Münster, D-48149 Münster, Germany
[35] Dept. of Physics, Drexel University, 3141 Chestnut Street, Philadelphia, PA 19104, USA
[36] Dept. of Physics and Astronomy, Stony Brook University, Stony Brook, NY 11794-3800, USA
[37] Dept. of Physics, Sungkyunkwan University, Suwon 16419, Republic of Korea
[38] Dept. of Physics and Astronomy, Michigan State University, East Lansing, MI 48824, USA
[39] Vrije Universiteit Brussel (VUB), Dienst ELEM, B-1050 Brussels, Belgium
[40] Dept. of Astronomy and Astrophysics, Pennsylvania State University, University Park, PA 16802, USA
[41] Dept. of Physics and Astronomy, University of Alabama, Tuscaloosa, AL 35487, USA
[42] Centre for Cosmology, Particle Physics and Phenomenology—CP3, Université catholique de Louvain, Louvain-la-Neuve, Belgium
[43] Karlsruhe Institute of Technology, Institute of Experimental Particle Physics, D-76021 Karlsruhe, Germany
[44] Dept. of Physics, Southern University, Baton Rouge, LA 70813, USA
[45] Institute of Physics, Academia Sinica, Taipei, 11529, Taiwan
[46] Institut für Physik, Humboldt-Universität zu Berlin, D-12489 Berlin, Germany
[47] Dept. of Astronomy, University of Wisconsin–Madison, Madison, WI 53706, USA
[48] Dept. of Physics, Engineering Physics, and Astronomy, Queen's University, Kingston, ON K7L 3N6, Canada
[49] Dept. of Physics, University of Alberta, Edmonton, Alberta, T6G 2E1, Canada
[50] Dept. of Physics and The International Center for Hadron Astrophysics, Chiba University, Chiba 263-8522, Japan
[51] CTSPS, Clark-Atlanta University, Atlanta, GA 30314, USA
[52] Dept. of Physics, University of Texas at Arlington, 502 Yates St., Science Hall Rm 108, Box 19059, Arlington, TX 76019, USA
[53] Department of Physics and Astronomy, UCLA, Los Angeles, CA 90095, USA
[54] Dept. of Physics, Yale University, New Haven, CT 06520, USA
[55] Department of Physics, Mercer University, Macon, GA 31207-0001, USA
[56] Dept. of Physics and Astronomy, University of Gent, B-9000 Gent, Belgium
[57] Dept. of Physics and Astronomy, University of Alaska Anchorage, 3211 Providence Dr., Anchorage, AK 99508, USA
[58] Department of Physics and Astronomy, University of Utah, Salt Lake City, UT 84112, USA
[59] Dept. of Physics, University of Oxford, Parks Road, Oxford OX1 3PU, UK
[60] Dept. of Physics, University of Wisconsin, River Falls, WI 54022, USA
[61] Institute of Basic Science, Sungkyunkwan University, Suwon 16419, Republic of Korea
Received 2022 July 5; revised 2022 August 17; accepted 2022 August 17; published 2022 October 12

Abstract

The majority of astrophysical neutrinos have undetermined origins. The IceCube Neutrino Observatory has observed astrophysical neutrinos but has not yet identified their sources. Blazars are promising source candidates,

[62] also at Università di Padova, I-35131 Padova, Italy.
[63] also at Earthquake Research Institute, University of Tokyo, Bunkyo, Tokyo 113-0032, Japan.

but previous searches for neutrino emission from populations of blazars detected in $\gtrsim$GeV gamma rays have not observed any significant neutrino excess. Recent findings in multimessenger astronomy indicate that high-energy photons, coproduced with high-energy neutrinos, are likely to be absorbed and reemitted at lower energies. Thus, lower-energy photons may be better indicators of TeV–PeV neutrino production. This paper presents the first time-integrated stacking search for astrophysical neutrino emission from MeV-detected blazars in the first Fermi Large Area Telescope low energy (1FLE) catalog using ten years of IceCube muon–neutrino data. The results of this analysis are found to be consistent with a background-only hypothesis. Assuming an E^{-2} neutrino spectrum and proportionality between the blazars MeV gamma-ray fluxes and TeV–PeV neutrino flux, the upper limit on the 1FLE blazar energy-scaled neutrino flux is determined to be 1.64×10^{-12} TeV cm^{-2} s^{-1} at 90% confidence level. This upper limit is approximately 1% of IceCube's diffuse muon–neutrino flux measurement.

Key words: Particle astrophysics – High energy astrophysics – Cosmic ray sources

1. Introduction

High-energy cosmic rays have been observed arriving at Earth (Abbasi et al. 2016; Zyla et al. 2020; Abreu et al. 2021), but their origins have yet to be determined. The observation of these particles with PeV and higher energies implies the existence of powerful astrophysical particle accelerators; however, the nature and locations of these objects remain uncertain. Charged particles with energies smaller than $\sim 10^{19}$ eV traveling through the universe are deflected by interstellar and intergalactic magnetic fields (Arámburo-García et al. 2021), thereby making localization of cosmic ray sources difficult.

In contrast to charged particles, photons and neutrinos travel along a straight path from their sources making them useful messengers for observing cosmic ray accelerators. Unlike photons, which can be produced by leptonic or hadronic processes, the production of a large neutrino flux requires the presence of a hadronic component. Therefore, the emission of neutrinos is generally considered a strong sign of cosmic ray acceleration. Additionally, photon attenuation probability increases rapidly with energy $\gtrsim$30 GeV over cosmic distances (Ajello et al. 2017). On the other hand, the neutrino's small interaction cross section allows it to travel great distances without absorption making them effective at probing distances that photons cannot.

These same properties necessitate a large detector volume to effectively observe neutrinos, especially those of astrophysical origin that have a relatively small flux compared to solar and atmospheric neutrinos. The IceCube Neutrino Observatory (hereafter IceCube) is a cubic-kilometer Cherenkov light detector located at the geographic South Pole (Aartsen et al. 2017a). In 2013, IceCube discovered the existence of a flux of high-energy, astrophysical neutrinos (Aartsen et al. 2013). No sources of these astrophysical neutrinos have yet been found with post-trial significance exceeding 5σ.

Active galactic nuclei (AGN) are highly energetic objects that have long been theorized to be potential sites for particle acceleration and neutrino production (Halzen & Zas 1997). The accretion of surrounding matter onto a supermassive black hole creates an ideal environment for acceleration and interaction of cosmic particles. In some AGN, particles may additionally be accelerated along a narrow, relativistic jet. Four AGN make up the most significant combined group of sources in an analysis of 10 yr of IceCube data (Aartsen et al. 2020a); among these are the Seyfert and starburst galaxy NGC 1068 and blazar TXS 0506+056.

This blazar, TXS 0506+056, is the first object to show evidence for astrophysical neutrino emission (Aartsen et al. 2018a, 2018b) with greater than 3σ significance. Blazars are AGN that have a relativistic jet directed toward Earth, providing a potentially greater observed flux of accelerated particles (Urry & Padovani 1995). Current observations of blazars are unable to distinguish between leptonic, hadronic, and mixed emission scenarios (Böttcher et al. 2013; Cerruti et al. 2019). When a hadronic component is included, a neutrino counterpart is expected alongside the photon production; hence, detections of neutrinos from blazars can help characterize their makeup.

Previous IceCube analyses (Aartsen et al. 2017b; Huber 2019), though, have not found significant astrophysical neutrino emission from blazars in the 2 yr Fermi Large Area Telescope (LAT) AGN catalog (2LAC; Ackermann et al. 2011) and the Fermi-LAT third high energy source catalog (3FHL; Ajello et al. 2017). Recent theoretical hypotheses (Murase et al. 2016) suggest that photons produced alongside astrophysical neutrinos in cosmic accelerators will be more effectively observed at reduced energies due to processes that attenuate high-energy photons. At the source, high-energy gamma rays are unlikely to escape their environment without being absorbed, for example by pair-production with other gamma rays, inverse Compton scattering, or synchrotron cooling (Mannheim et al. 1991, 2000). Photons that do escape their source with $\gtrsim$ GeV energies have a high probability of cascading to lower energies via interaction with extragalactic background light and the cosmic microwave background as they travel from their source (Berezinskii & Smirnov 1975). These processes lead not only to an increased observed electromagnetic flux at MeV energies but also to the possibility for some neutrino sources to be unobserved in the GeV–TeV energy range (Murase et al. 2016). In addition, blazar spectral energy distributions tend to peak in the MeV regime, especially for the most luminous objects (Fossati et al. 1998; Gao et al. 2017; Ojha et al. 2019). For these reasons, MeV photons could be more effective indicators of TeV–PeV neutrinos.

2. Sources

This analysis searches for correlation between IceCube neutrinos and 137 blazars in the first catalog of Fermi-LAT sources detected below 100 MeV (first Fermi-LAT low energy, hereafter 1FLE; Principe et al. 2018). These blazars are mapped in equatorial coordinates in Figure 1 with marker sizes proportional to each blazar's respective 30–100 MeV photon energy flux. The LAT on board the Fermi Gamma-ray Space Telescope (Fermi) observes the universe in gamma rays of energies from 20 MeV to over 300 GeV, its most sensitive energies falling in the GeV band (Atwood et al. 2009). The 1FLE catalog was created using a wavelet transform method, to localize sources and fit for fluxes, which is described in detail

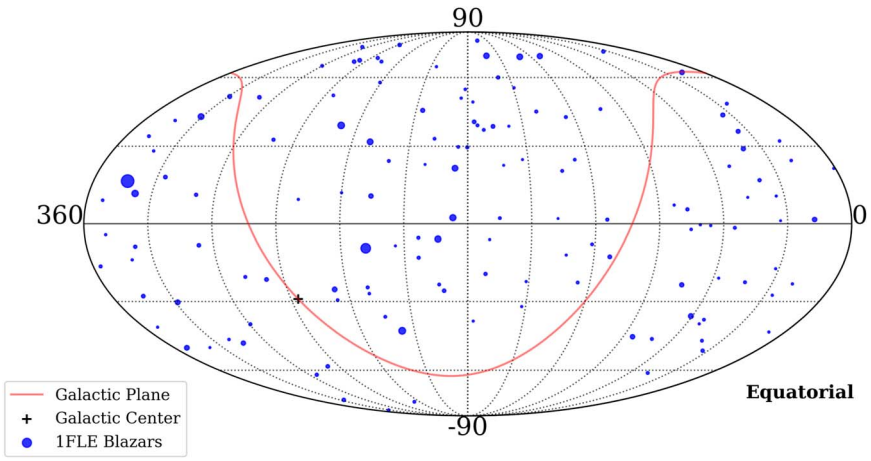

Figure 1. Sky map showing locations of 1FLE blazars used as sources in this analysis in equatorial coordinates. The marker size for each blazar is proportional to its MeV gamma-ray flux. Also shown are the Galactic center (black cross) and Galactic plane (red line) for reference. Note that, despite some sources' proximities to the Galactic plane, all blazars are extragalactic.

in Principe et al. (2018). The blazars used in this analysis are classified as either flat-spectrum radio quasars (FSRQs) or BL Lacertae objects (BL Lac objects). These classifications are obtained from each blazar's respective source association in the 10 yr Fermi-LAT data release (4FGL-DR2; Abdollahi et al. 2020) in order to have the most updated identification. It is important to note, however, that blazars are not split into separate classifications for use in this analysis. While there are blazars shared between the 1FLE catalog and the catalogs used in previous IceCube blazar stacking analyses (2LAC and 3FHL), the number of sources and the photon flux energy range differentiate this analysis from previous, similar ones. A brief overview of these quantities in this analysis and those previously mentioned is presented in Table 1.

The 30–100 MeV photon energy range of the 1FLE catalog is below the peak sensitivity of the Fermi-LAT instrument. In general, this leads to a lower precision on measured quantities. For instance, the 1FLE catalog localizes sources within error radii of about 0°.25 (Principe et al. 2018). In comparison, 4FGL sources, which are localized using photons where Fermi-LAT is more sensitive above 100 MeV, have error radii that tend to be around 0°.05 (varying up to about 0°.5 and down to about 0°.005; Abdollahi et al. 2020). Despite these greater uncertainties in the 1FLE catalog, the locations of the blazars do not vary greatly from their 4FGL associations. Additionally, the 1FLE source detection methods are designed to detect faint sources while also limiting source confusion (see Principe et al. 2018 for full explanation). This specific focus of the 1FLE catalog on detection efficiency in the 30–100 MeV photon energy range makes it a good choice for this analysis. Of further importance is the fact that the source localization errors are still smaller or similar to the IceCube pointing resolution, so they do not contribute significant error when correlating with IceCube events. All this considered, without instruments that are sensitive to the MeV range of the electromagnetic spectrum, the 1FLE catalog acts as an important bridge over previously unexplored energies. A full list of source blazars used in this analysis and relevant quantities can be found in Appendix.

Table 1
Comparison of IceCube Blazar Stacking Analyses

Analysis	Source Catalog	Total Number of Blazars	Flux Weight Energy Range (GeV)
Aartsen et al. (2017b)	2LAC	862	0.1–100
Huber (2019)	3FHL	745	...
This work	1FLE	137	0.03-0.1

Note. Overview of two blazar stacking analyses is shown in addition to this work. In comparison to the 137 1FLE blazars studied in this analysis, 862 blazars from the 2LAC (Ackermann et al. 2011) catalog were analyzed with flux weights in the 0.1–100 GeV energy range, and 745 blazars from the 3FHL (Ajello et al. 2017) catalog were analyzed without flux weights.

3. Data

The IceCube detector (Aartsen et al. 2017a) consists of 5160 digital optical modules (DOMs) arranged in a cubic kilometer array of Antarctic ice. The main component of each DOM is a photomultiplier tube that collects the light created by relativistic particles traveling through the ice. These particles are produced as byproducts of neutrino interactions and emit Cherenkov radiation when traveling faster than the local speed of light through the ice. IceCube can detect all flavors of neutrinos, but no distinction can be made between neutrino (ν) and antineutrino ($\bar{\nu}$) except in rare cases such as the Glashow resonance (Aartsen et al. 2021a). IceCube observes two main event topologies at energies >100 GeV: cascades and tracks. Cascade events appear as a near-spherical propagation of light resulting from neutral-current neutrino interactions of all flavors or from charged-current (CC) interactions of electron- and tau-neutrinos ($\nu_e\bar{\nu}_e$ and $\nu_\tau\bar{\nu}_\tau$, respectively). At energies greater than a few hundred TeV, the CC $\nu_\tau\bar{\nu}_\tau$ interaction can produce a double-cascade light signature as the resulting tau particle travels a distance resolvable by IceCube (Aartsen et al. 2016). The data used in this analysis are track events. The track topology mostly results from the CC interactions of muon–neutrinos ($\nu_\mu + \bar{\nu}_\mu$); the muon produced in these interactions travels an order of several kilometers through the Antarctic ice as it loses energy, thereby depositing light in a linear pattern. This allows for tracks to be reconstructed with an angular resolution of $\lesssim 1°$ for neutrinos with energies $\gtrsim 1$ TeV (Aartsen et al. 2020a). This angular resolution is smaller than that of cascade events, which makes track events favored for point-source searches.

Table 2
Stacking Analysis Results for 1FLE Blazars

Weighting Scheme	TS	n_s	Energy-scaled Neutrino Flux UL (TeV cm^{-2} s^{-1} at 1 TeV)			
			$\gamma = 2.0$	$\gamma = 2.37$	$\gamma = 2.5$	$\gamma = 3.0$
Equal	0	0	2.27×10^{-12}	1.48×10^{-11}	2.48×10^{-11}	9.72×10^{-11}
Flux	0	0	1.64×10^{-12}	9.98×10^{-12}	1.65×10^{-11}	6.07×10^{-11}

Note. The 90% confidence level upper limits on stacked, energy-scaled neutrino ($\nu_\mu + \bar{\nu}_\mu$) flux are shown for several assumed spectral indices at a reference energy of 1 TeV, along with the best-fit TS and n_s, for each weighting scheme. These upper limits do not include systematic uncertainties.

The data set used to perform this analysis contains 1134451 IceCube track events collected between 2008 April 6 and 2018 July 8 from the entire sky. As the estimated angular uncertainty for each individual event does not include systematic uncertainties, a minimum angular uncertainty of 0°.2 is applied (Aartsen et al. 2020a). A majority of this data set is background events created by atmospheric neutrinos and muons resulting from cosmic ray interactions with Earth's atmosphere. Significant reduction of this background is achieved in the northern hemisphere due to shielding from muons by the Earth. Further details about the data set and event selection methods may be found in Abbasi et al. (2021).

4. Analysis Methods

This analysis uses a well-defined (Braun et al. 2008; Aartsen et al. 2017b, 2020b), unbinned, maximum likelihood method, which makes use of location and energy information to determine the possible correlation between IceCube neutrinos and 1FLE blazars. It is a stacked search that looks for cumulative neutrino emission from the source list as a whole, rather than individually. This time-independent analysis assumes steady emission from the sources as opposed to searching for transient emission. The likelihood, $\mathcal{L}$—which is a function of two free variables, the number of signal events, n_s, and the neutrino spectral index, γ—is defined in Equation (1). This likelihood can then be maximized to obtain a best-fit n_s and γ.

$$\mathcal{L}(n_s, \gamma) = \prod_i^N \left(\frac{n_s}{N} S_i + \left(1 - \frac{n_s}{N}\right) B_i \right). \quad (1)$$

The value N is the total number of events in the data sample. The likelihood consists of two PDFs for each event, i: one for signal, S_i, and one for background, B_i. The PDFs each consist of a spatial and an energy factor that correlate each event with a source.

As this is a stacked search, S_i is the weighted sum over every source j such that $S_i = \sum_j^M w_j R_j S_i^j$ for M total sources. The weight of each source consists of a detector acceptance weight, R_j, based on the effective area at the source location and a source weighting scheme, w_j, based on a chosen emission hypothesis. These weights are normalized such that $\sum_j^M w_j R_j = 1$; for more details, see Aartsen et al. (2020b). The two source weighting schemes chosen for use in this analysis are equally weighted sources (referred to as equal weights), and sources weighted by their integrated photon energy fluxes in the 30–100 MeV range (referred to as flux weights).

A test statistic (TS) is then constructed, as in Equation (2), to compare the best-fit signal hypothesis to a background-only hypothesis that is characterized by having zero signal events. This TS is used to determine the significance of the correlation in the form of a p-value, defined as the probability that the observed TS is a result of background fluctuations.

$$\mathrm{TS} = -2 \log \left(\frac{\mathcal{L}(n_s = 0)}{\mathcal{L}(n_s, \gamma)} \right). \quad (2)$$

As mentioned in Section 3, the data sample is background dominated. IceCube's location at the geographic South Pole leads to a decl.-dependent detector acceptance and event rate. Therefore, a model-independent background estimation is obtained by randomizing the R.A. of data events. This background estimation is repeated many times to create a distribution to which the observed TS may be compared in order to determine the p-value.

5. Results

The best-fit number of signal events for both source weighting hypotheses is found to be zero; hence our observations are consistent with the background-only hypothesis. Upper limits (ULs) are set on the energy-scaled neutrino flux ($E^2 dN/dE$) for various, assumed neutrino spectral indices and do not include systematic uncertainties. Such systematic uncertainties arise from DOM efficiency, absorption or scattering of photons in the ice, and photonuclear interaction models; the total systematic uncertainty on neutrino fluxes is approximately 11% (Aartsen et al. 2017). The results of this analysis are summarized in Table 2. Additionally, Figure 2 shows differential ULs on energy-scaled neutrino flux for an E^{-2} neutrino spectrum in bins of energy. The range of energies shown in the figure is that which contributes 90% of the integrated sensitivity for each weighting scheme.

Figure 3 compares the UL of this analysis under the flux-weighted source hypothesis to the astrophysical diffuse $\nu_\mu + \bar{\nu}_\mu$ flux from Abbasi et al. (2022). The UL of the analysis presented in this paper is on the per-flavor neutrino flux, which for a track data set, such as the one used here, can be closely approximated as a $\nu_\mu + \bar{\nu}_\mu$ flux. The spectral index of the UL shown in Figure 3 is chosen to be 2.37 to match the best-fit spectral index of the compared diffuse measurement. By extending this limit to lower energies, it is also naively compared to the sum of 30–100 MeV photon energy fluxes from the 1FLE blazars used in this analysis. At around this spectral index and smaller, the hadronic component of the MeV gamma-ray flux may be constrained by the neutrino flux ULs presented here. The specifics of this constraint and its viability are dependent on the choice of blazar flux model but are beyond the scope of this paper.

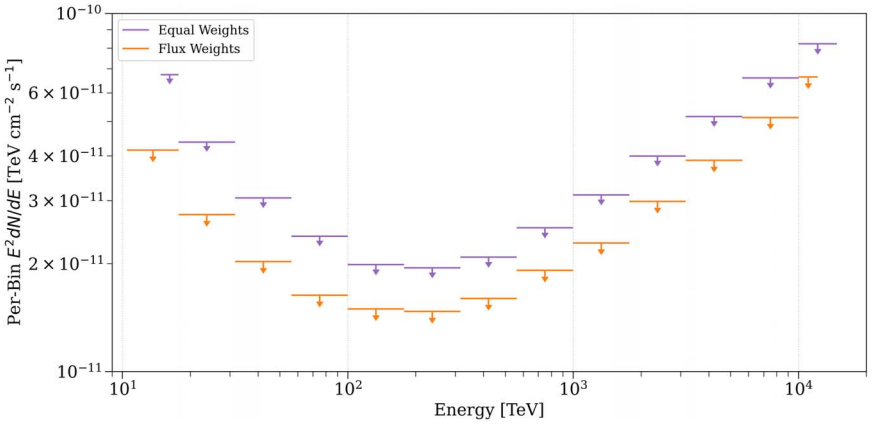

Figure 2. 90% confidence level upper limits on energy-scaled neutrino ($\nu_\mu + \bar{\nu}_\mu$) flux from 1FLE blazars in four differential bins per decade of energy. These limits correspond to an E^{-2} neutrino spectrum within each energy bin and do not include systematic uncertainties. The overall energy range is that which contributed 90% of the total sensitivity for each respective weighting scheme.

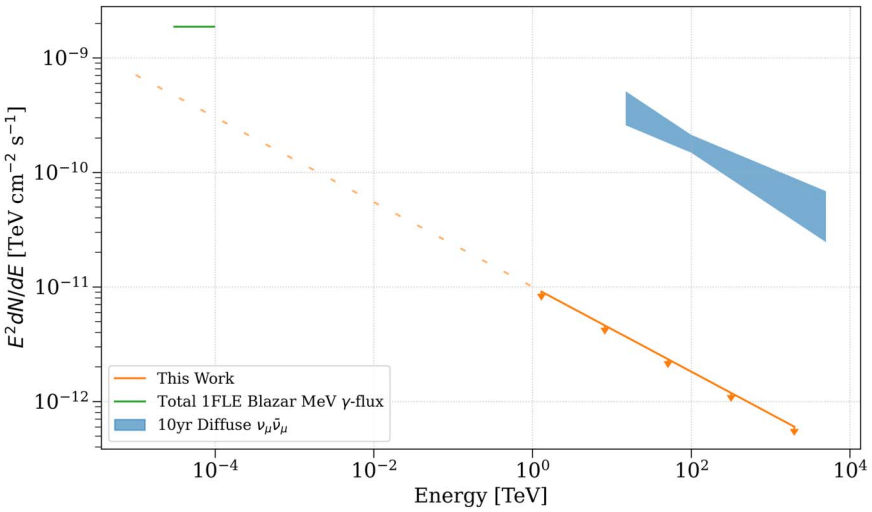

Figure 3. 90% confidence level upper limit on energy-scaled neutrino ($\nu_\mu + \bar{\nu}_\mu$) flux from 1FLE blazars assuming a simple power law (orange), which is 1.0% of the diffuse flux measurement from Abbasi et al. (2022; blue, shown as a 68% confidence level band). This upper limit does not include systematic uncertainties. The spectral index shown here, $\gamma = 2.37$, is the best fit of this diffuse measurement. The solid orange line shows the limit within the energy range that contributes 90% of the total sensitivity. The dashed line extrapolates this limit to lower energies. The green line shows the sum of integrated gamma-ray fluxes between 30 and 100 MeV for 1FLE blazars, which are used as source weights in obtaining the shown upper limit. Considering the relationship between this total flux and the limit from this analysis in the 30–100 MeV range, in conjunction with a gamma-ray model, could offer insight into the contribution of hadronic interactions to the observed blazar flux distribution.

6. Conclusions

A stacking analysis searching for astrophysical neutrino production from 137 blazars in the Fermi-LAT 1FLE catalog using 10 yr of IceCube muon–neutrino data was presented. Observations were found, via the described methods, to be consistent with the background-only hypothesis for both equal and flux source weighting schemes. ULs were set on the energy-scaled neutrino flux from these blazars for both source weightings and various assumed spectral indices. Under the 30–100 MeV photon flux (equal) weighting scheme and for a spectral index of 2.37, the UL from this analysis is approximately 0.86%–1.2% (1.3%–1.8%) of the most recent diffuse $\nu_\mu + \bar{\nu}_\mu$ flux measurement; this diffuse measurement uses IceCube track events observed in the northern celestial hemisphere from 2009 through 2018.

The two blazar stacking analyses previously performed by IceCube and included in Table 1 produced less stringent constraints on the diffuse astrophysical neutrino flux. It is important to consider, however, the differences between the analyses. In addition to the number of blazars and the energy range of the gamma-ray fluxes used to correlate with neutrino emission, each analysis uses a different set of IceCube data and compares to a different diffuse astrophysical neutrino flux. Each diffuse flux was measured using different sets of data and with varying methods; therefore, comparisons of constraints on these fluxes should be made with caution. Aartsen et al. (2017b) uses IceCube data collected from the whole sky from 2009 to 2012. It reports an UL for 862 2LAC blazars with GeV gamma-ray flux weighting of 7% of the diffuse flux from Aartsen et al. (2015). The Aartsen et al. (2015) analysis performs a combined, all-sky fit of six diffuse flux measurements, which include both cascade and track events from data-taking periods between 2009 and 2013. The best-fit spectral index from that analysis—which was also used to calculate the 2LAC UL—is 2.5. The analysis of 3FHL blazars (Huber 2019) compares its UL to the diffuse $\nu_\mu + \bar{\nu}_\mu$ flux from Haack & Wiebusch (2017), which uses IceCube track events observed in

the northern sky from 2009 through 2017; it finds a best-fit spectral index of 2.19. Huber (2019) uses a sample of IceCube events from the northern hemisphere and reports an UL for 745 northern-sky, GeV-detected 3FHL blazars of 9.7%–13.9% of the diffuse flux for all blazar classes; the same analysis finds the UL for 101 FSRQs alone to be 2.9%–3.8% of the diffuse flux.

For a more direct comparison with Huber (2019), the UL from the work presented in this paper is compared to the Haack & Wiebusch (2017) diffuse flux measurement. This UL for 137 1FLE blazars (of which 106 are FSRQs) with MeV gamma-ray flux weighting and an assumed spectral index of 2.19 is 1.1%–1.9% of the Haack & Wiebusch (2017) diffuse flux. It is also worth noting that TXS 0506+056, which showed significant evidence for astrophysical neutrino emission (Aartsen et al. 2018a, 2018b), is classified as a BL Lac object, and its 30–100 MeV photon flux is roughly average in the 1FLE catalog. While it is possible that the 30–100 MeV photon energy range is not strongly correlated with emission of TeV–PeV astrophysical neutrinos in blazars, this analysis and the comparisons presented here cannot distinguish whether MeV or GeV photons have a stronger correlation, and further exploration is encouraged.

It should be noted that this analysis contains limitations that result from the 1FLE catalog lying outside of Fermi-LAT's most sensitive energy range. This results in fewer detected objects. Also, the localization and flux precisions are worse than those in the most sensitive energies of this instrument, but are not accounted for with the methods of this analysis. Nevertheless, this analysis is a first search for astrophysical neutrino emission from 30–100 MeV gamma-ray-detected blazars and should lend itself as motivation for future studies into the low-energy gamma-ray band. Future electromagnetic observations in the MeV band will provide a larger number of sources with higher precision allowing for an updated analysis similar to the one presented here to be performed. For example, AMEGO-X (Fleischhack 2021) and e-ASTROGAM (De Angelis et al. 2018) plan to offer much improved sensitivities in the MeV energy range and even down to a few hundred keV. Future analyses will also benefit from additional neutrino observations from upcoming improvements to neutrino observational capabilities, such as with IceCube-Gen2 (Aartsen et al. 2021).

The IceCube collaboration acknowledges the significant contributions to this manuscript from Michael A. Campana. The authors would like to acknowledge support as follows: from the USA, U.S. National Science Foundation (Office of Polar Programs), U.S. National Science Foundation (Physics Division), U.S. National Science Foundation (EPSCoR), Wisconsin Alumni Research Foundation, Center for High Throughput Computing (CHTC) at the University of Wisconsin (Madison), Open Science Grid (OSG), Extreme Science and Engineering Discovery Environment (XSEDE), Frontera computing project at the Texas Advanced Computing Center, U.S. Department of Energy-National Energy Research Scientific Computing Center, Particle astrophysics research computing center at the University of Maryland, Institute for Cyber-Enabled Research at Michigan State University, and Astroparticle physics computational facility at Marquette University; from Belgium, Funds for Scientific Research (FRS-FNRS and FWO), FWO Odysseus and Big Science programmes, and Belgian Federal Science Policy Office (Belspo); from Germany, Bundesministerium für Bildung und Forschung (BMBF), Deutsche Forschungsgemeinschaft (DFG), Helmholtz Alliance for Astroparticle Physics (HAP), Initiative and Networking Fund of the Helmholtz Association, Deutsches Elektronen Synchrotron (DESY), and High Performance Computing cluster of the RWTH Aachen; from Sweden, Swedish Research Council, Swedish Polar Research Secretariat, Swedish National Infrastructure for Computing (SNIC), and Knut and Alice Wallenberg Foundation; from Australia, Australian Research Council; from Canada, Natural Sciences and Engineering Research Council of Canada, Calcul Québec, Compute Ontario, Canada Foundation for Innovation, WestGrid, and Compute Canada; from Denmark, Villum Fonden and Carlsberg Foundation; from New Zealand, Marsden Fund; from Japan, Japan Society for Promotion of Science (JSPS) and Institute for Global Prominent Research (IGPR) of Chiba University; from Korea, National Research Foundation of Korea (NRF); from Switzerland, Swiss National Science Foundation (SNSF); and from the United Kingdom, Department of Physics at the University of Oxford.

Appendix
Source List

Table 3 contains a list of the 137 blazars analyzed in this work along with relevant quantities.

Table 3
List of Blazars from the 1FLE Catalog That Are Used in This Analysis

Name	4FGL Association	Class	R.A. (°)	Decl. (°)	30–100 MeV Energy Flux (10^{-12} erg cm^{-2} s^{-1})	Redshift[a]
1FLE J0003+2114	4FGL J0001.5+2113	fsrq	0.8	21.2	8.2 ± 2.7	1.11
1FLE J0036-4236	4FGL J0030.3-4224	fsrq	9.2	−42.6	8.3 ± 2.8	0.5
1FLE J0109+0136	4FGL J0108.6+0134	fsrq	17.3	1.6	34 ± 10	2.1
1FLE J0105+6233	4FGL J0109.7+6133	fsrq	16.5	62.6	35 ± 10	0.78
1FLE J0111+3207	4FGL J0112.8+3208	fsrq	18.0	32.1	10.5 ± 3.5	0.6
1FLE J0117+2420	4FGL J0115.8+2519	bll	19.4	24.3	10.4 ± 3.4	0.36
1FLE J0119-2300	4FGL J0118.9-2141	fsrq	19.8	−23.0	8.5 ± 2.8	1.16
1FLE J0136+4752	4FGL J0137.0+4751	fsrq	24.2	47.9	13.8 ± 4.6	0.86
1FLE J0144-2728	4FGL J0145.0-2732	fsrq	26.2	−27.5	8.4 ± 2.8	1.15
1FLE J0206-1705	4FGL J0205.0-1700	fsrq	31.6	−17.1	7.8 ± 2.6	1.74
1FLE J0213-5047	4FGL J0210.7-5101	fsrq	33.4	−50.8	19.1 ± 5.8	1.0
1FLE J0215+1034	4FGL J0211.2+1051	bll	33.8	10.6	7.4 ± 2.4	…
1FLE J0221+7403	4FGL J0217.4+7352	fsrq	35.4	74.1	18.9 ± 5.7	2.37
1FLE J0213+0107	4FGL J0217.8+0144	fsrq	33.3	1.1	5.8 ± 1.9	1.72
1FLE J0221+3604	4FGL J0221.1+3556	fsrq	35.4	36.1	26.3 ± 7.9	0.94

Table 3
(Continued)

Name	4FGL Association	Class	R.A. (°)	Decl. (°)	30–100 MeV Energy Flux (10^{-12} erg cm^{-2} s^{-1})	Redshift[a]
1FLE J0219+4256	4FGL J0222.6+4302	bll	34.8	42.9	28.2 ± 8.5	0.44
1FLE J0238+2900	4FGL J0237.8+2848	fsrq	39.6	29.0	29.4 ± 8.9	1.21
1FLE J0238+1638	4FGL J0238.6+1637	bll	39.5	16.6	17.3 ± 5.2	0.94
1FLE J0246-4621	4FGL J0245.9-4650	fsrq	41.7	−46.4	13.6 ± 4.5	1.38
1FLE J0254-2221	4FGL J0252.8-2219	fsrq	43.6	−22.4	13.8 ± 4.6	1.43
1FLE J0309+1002	4FGL J0309.0+1029	fsrq	47.5	10.0	6.6 ± 2.2	0.86
1FLE J0304-6121	4FGL J0309.9-6058	fsrq	46.1	−61.4	14.3 ± 4.7	1.48
1FLE J0325+2204	4FGL J0325.7+2225	fsrq	51.5	22.1	11.0 ± 3.7	2.07
1FLE J0329-3724	4FGL J0334.2-3725	bll	52.3	−37.4	13.4 ± 4.4	⋯
1FLE J0331-3909	4FGL J0334.2-4008	bll	52.9	−39.2	7.8 ± 2.6	1.36
1FLE J0339-0133	4FGL J0339.5-0146	fsrq	54.8	−1.6	13.9 ± 4.6	0.85
1FLE J0349-2045	4FGL J0349.8-2103	fsrq	57.4	−20.8	7.2 ± 2.4	2.94
1FLE J0403-3554	4FGL J0403.9-3605	fsrq	60.8	−35.9	40.8 ± 9.1	1.42
1FLE J0424-0042	4FGL J0423.3-0120	fsrq	66.1	−0.7	7.6 ± 2.5	0.92
1FLE J0443-0024	4FGL J0442.6-0017	fsrq	71.0	−0.4	7.6 ± 2.5	0.84
1FLE J0448-4535	4FGL J0455.7-4617	fsrq	72.2	−45.6	14.6 ± 4.8	0.86
1FLE J0456-2322	4FGL J0457.0-2324	fsrq	74.2	−23.4	30.3 ± 9.1	1.0
1FLE J0500-0209	4FGL J0501.2-0158	fsrq	75.2	−2.2	10.1 ± 3.3	2.29
1FLE J0506+0528[b]	4FGL J0509.4+0542	bll	76.7	5.5	16.9 ± 5.6	⋯
1FLE J0531+0707	4FGL J0532.6+0732	fsrq	82.8	7.1	8.0 ± 2.6	1.25
1FLE J0538-4438	4FGL J0538.8-4405	bll	84.5	−44.6	32.7 ± 9.9	0.89
1FLE J0649+4529	4FGL J0654.4+4514	fsrq	102.4	45.5	12.8 ± 4.2	0.93
1FLE J0721+7121	4FGL J0721.9+7120	bll	110.4	71.4	46 ± 10	0.13
1FLE J0729-1230	4FGL J0730.3-1141	fsrq	112.4	−12.5	22.9 ± 6.9	1.59
1FLE J0738+0133	4FGL J0739.2+0137	fsrq	114.5	1.6	15.9 ± 5.3	0.19
1FLE J0805-0743	4FGL J0808.2-0751	fsrq	121.4	−7.7	12.5 ± 4.1	1.84
1FLE J0818+4202	4FGL J0818.2+4222	bll	124.7	42.0	14.5 ± 4.8	0.53
1FLE J0823-2228	4FGL J0825.9-2230	bll	125.9	−22.5	13.1 ± 4.3	0.91
1FLE J0827+2440	4FGL J0830.8+2410	fsrq	126.8	24.7	11.4 ± 3.8	0.94
1FLE J0841+7056	4FGL J0841.3+7053	fsrq	130.4	70.9	54 ± 12	2.22
1FLE J0852-1149	4FGL J0850.1-1212	fsrq	133.2	−11.8	7.3 ± 2.4	0.57
1FLE J0855+2014	4FGL J0854.8+2006	bll	134.0	20.2	13.4 ± 4.4	0.31
1FLE J0910+0159	4FGL J0909.1+0121	fsrq	137.6	2.0	5.9 ± 2.0	1.02
1FLE J0921+4425	4FGL J0920.9+4441	fsrq	140.4	44.4	15.2 ± 5.0	2.19
1FLE J0957+5503	4FGL J0957.6+5523	fsrq	149.3	55.1	8.8 ± 2.9	0.9
1FLE J1005-2205	4FGL J1006.7-2159	fsrq	151.3	−22.1	7.6 ± 2.5	0.33
1FLE J1008-3201	4FGL J1008.8-3139	bll	152.0	−32.0	7.7 ± 2.5	⋯
1FLE J1011+2442	4FGL J1012.7+2439	fsrq	152.8	24.7	6.6 ± 2.2	1.8
1FLE J1031+6001	4FGL J1031.6+6019	fsrq	158.0	60.0	17.7 ± 5.3	1.23
1FLE J1030+3811	4FGL J1032.6+3737	bll	157.6	38.2	7.0 ± 2.3	⋯
1FLE J1047+7131	4FGL J1048.4+7143	fsrq	161.9	71.5	51 ± 11	1.15
1FLE J1049+2227	4FGL J1054.5+2211	bll	162.3	22.5	6.2 ± 2.1	⋯
1FLE J1059+0208	4FGL J1058.4+0133	bll	164.9	2.1	13.2 ± 4.4	0.89
1FLE J1100+8117	4FGL J1058.5+8115	fsrq	165.1	81.3	17.7 ± 5.3	0.71
1FLE J1105+3807	4FGL J1104.4+3812	bll	166.3	38.1	24.4 ± 7.4	0.03
1FLE J1118-0558	4FGL J1121.4-0553	fsrq	169.7	−6.0	6.1 ± 2.0	1.3
1FLE J1125-1907	4FGL J1127.0-1857	fsrq	171.4	−19.1	17.7 ± 5.3	1.05
1FLE J1125+3639	4FGL J1127.8+3618	fsrq	171.4	36.7	13.1 ± 4.3	0.88
1FLE J1138+3832	4FGL J1131.0+3815	fsrq	174.7	38.5	13.4 ± 4.4	1.73
1FLE J1145+4001	4FGL J1146.9+3958	fsrq	176.5	40.0	21.6 ± 6.5	1.09
1FLE J1148-3800	4FGL J1147.0-3812	bll	177.0	−38.0	7.2 ± 2.4	1.05
1FLE J1147+4836	4FGL J1153.4+4931	fsrq	176.9	48.6	7.8 ± 2.6	0.33
1FLE J1201+2934	4FGL J1159.5+2914	fsrq	180.3	29.6	15.4 ± 5.1	0.72
1FLE J1206+5421	4FGL J1208.9+5441	fsrq	181.6	54.4	10.1 ± 3.4	1.34
1FLE J1219+2943	4FGL J1217.9+3007	bll	184.9	29.7	11.9 ± 3.9	0.13
1FLE J1216+5019	4FGL J1223.9+5000	fsrq	184.1	50.3	8.4 ± 2.8	1.07
1FLE J1224+2118	4FGL J1224.9+2122	fsrq	186.2	21.3	56 ± 13	0.44
1FLE J1227+0218	4FGL J1229.0+0202	fsrq	187.0	2.3	65 ± 14	0.16
1FLE J1247-2541	4FGL J1246.7-2548	fsrq	191.8	−25.7	20.5 ± 6.2	0.64
1FLE J1256-0545	4FGL J1256.1-0547	fsrq	194.0	−5.8	63 ± 14	0.54
1FLE J1256-2314	4FGL J1258.8-2219	fsrq	194.1	−23.2	13.4 ± 4.4	1.3
1FLE J1309+3302	4FGL J1310.5+3221	fsrq	197.4	33.0	12.5 ± 4.1	1.0
1FLE J1324+2247	4FGL J1321.1+2216	fsrq	201.1	22.8	6.0 ± 2.0	0.94
1FLE J1332-0518	4FGL J1332.0-0509	fsrq	203.2	−5.3	15.2 ± 5.0	2.15
1FLE J1333-1250	4FGL J1332.6-1256	fsrq	203.4	−12.8	16.0 ± 5.3	1.5
1FLE J1342+6530	4FGL J1338.0+6534	fsrq	205.6	65.5	8.7 ± 2.9	0.95
1FLE J1344+4456	4FGL J1345.5+4453	fsrq	206.2	44.9	27.3 ± 8.2	2.53
1FLE J1416-0818	4FGL J1419.4-0838	fsrq	214.1	−8.3	6.4 ± 2.1	⋯
1FLE J1427-4205	4FGL J1427.9-4206	fsrq	217.0	−42.1	77 ± 17	1.55
1FLE J1436+2409	4FGL J1436.9+2321	fsrq	219.2	24.2	14.3 ± 4.8	1.54
1FLE J1456-3612	4FGL J1457.4-3539	fsrq	224.2	−36.2	12.7 ± 4.2	1.42

Table 3
(Continued)

Name	4FGL Association	Class	R.A. (°)	Decl. (°)	30–100 MeV Energy Flux (10^{-12} erg cm^{-2} s^{-1})	Redshift[a]
1FLE J1503+1033	4FGL J1504.4+1029	fsrq	225.9	10.6	31.7 ± 9.6	1.84
1FLE J1512-0913	4FGL J1512.8-0906	fsrq	228.2	−9.2	156 ± 32	0.36
1FLE J1518-2422	4FGL J1517.7-2422	bll	229.7	−24.4	14.7 ± 4.9	0.05
1FLE J1522+3147	4FGL J1522.1+3144	fsrq	230.6	31.8	56 ± 12	1.49
1FLE J1518-2650	4FGL J1522.6-2730	bll	229.5	−26.8	10.3 ± 3.4	1.29
1FLE J1559+1149	4FGL J1555.7+1111	bll	239.9	11.8	7.8 ± 2.7	…
1FLE J1603+5734	4FGL J1604.6+5714	fsrq	240.8	57.6	12.2 ± 4.1	0.72
1FLE J1626-7732	4FGL J1617.9-7718	fsrq	246.7	−77.5	12.7 ± 4.2	1.71
1FLE J1625-2510	4FGL J1625.7-2527	fsrq	246.4	−25.2	38 ± 12	0.79
1FLE J1625-2926	4FGL J1626.0-2950	fsrq	246.4	−29.4	12.1 ± 4.0	0.82
1FLE J1636+3831	4FGL J1635.2+3808	fsrq	249.1	38.5	73 ± 16	1.81
1FLE J1703+6815	4FGL J1700.0+6830	fsrq	255.8	68.3	14.1 ± 4.8	0.3
1FLE J1720+0916	4FGL J1722.7+1014	fsrq	260.1	9.3	8.0 ± 2.7	0.73
1FLE J1739+5134	4FGL J1740.5+5211	fsrq	264.8	51.6	11.7 ± 3.9	1.38
1FLE J1735+7015	4FGL J1748.6+7005	bll	263.9	70.3	16.6 ± 5.5	0.77
1FLE J1753+7815	4FGL J1800.6+7828	bll	268.4	78.3	20.4 ± 6.2	0.68
1FLE J1827+6859	4FGL J1823.5+6858	bll	276.9	69.0	23.3 ± 7.0	…
1FLE J1831-5805	4FGL J1832.6-5658	bll	277.9	−58.1	21.2 ± 6.4	…
1FLE J1834-2116	4FGL J1833.6-2103	fsrq	278.6	−21.3	23.4 ± 7.1	2.51
1FLE J1838+6812	4FGL J1842.3+6810	fsrq	279.6	68.2	20.8 ± 6.3	0.47
1FLE J1845+3238	4FGL J1848.4+3217	fsrq	281.3	32.6	16.5 ± 5.5	0.8
1FLE J1914-2017	4FGL J1911.2-2006	fsrq	288.5	−20.3	14.2 ± 4.7	1.12
1FLE J1938-6215	4FGL J1941.3-6210	bll	294.5	−62.3	17.5 ± 5.3	…
1FLE J1958-3919	4FGL J1958.0-3845	fsrq	299.6	−39.3	16.1 ± 5.3	0.63
1FLE J2001+6556	4FGL J2007.2+6607	fsrq	300.3	65.9	14.1 ± 4.7	1.32
1FLE J2028+7651	4FGL J2022.5+7612	bll	307.2	76.9	16.4 ± 5.4	0.59
1FLE J2027-0805	4FGL J2025.6-0735	fsrq	306.8	−8.1	21.1 ± 6.4	1.39
1FLE J2035+1102	4FGL J2035.4+1056	fsrq	308.8	11.0	17.6 ± 5.3	0.6
1FLE J2039+5042	4FGL J2038.7+5117	fsrq	309.9	50.7	21.5 ± 6.5	1.69
1FLE J2056-4724	4FGL J2056.2-4714	fsrq	314.2	−47.4	31.3 ± 9.4	1.49
1FLE J2120-4549	4FGL J2126.3-4605	fsrq	320.2	−45.8	9.8 ± 3.3	1.67
1FLE J2144+1751	4FGL J2143.5+1743	fsrq	326.2	17.9	22.1 ± 6.7	0.21
1FLE J2141-7616	4FGL J2147.3-7536	fsrq	325.4	−76.3	19.9 ± 6.0	1.14
1FLE J2155-3018	4FGL J2151.8-3027	fsrq	328.9	−30.3	39 ± 12	2.35
1FLE J2209-8335	4FGL J2201.5-8339	fsrq	332.4	−83.6	11.5 ± 3.8	1.86
1FLE J2156+5102	4FGL J2201.8+5048	fsrq	329.2	51.0	27.5 ± 8.3	1.9
1FLE J2203+4214	4FGL J2202.7+4216	bll	330.8	42.2	57 ± 13	0.07
1FLE J2227-0838	4FGL J2229.7-0832	fsrq	337.0	−8.6	18.7 ± 5.6	1.56
1FLE J2231+1132	4FGL J2232.6+1143	fsrq	337.9	11.5	69 ± 15	1.04
1FLE J2232-4923	4FGL J2235.3-4836	fsrq	338.0	−49.4	6.8 ± 2.3	0.51
1FLE J2236+2807	4FGL J2236.3+2828	fsrq	339.2	28.1	9.2 ± 3.0	0.79
1FLE J2240-1340	4FGL J2236.5-1433	bll	340.1	−13.7	8.3 ± 2.7	…
1FLE J2251+4034	4FGL J2244.2+4057	fsrq	342.8	40.6	9.8 ± 3.3	1.17
1FLE J2256-2750	4FGL J2250.7-2806	bll	344.1	−27.8	22.4 ± 6.8	0.52
1FLE J2254+1617	4FGL J2253.9+1609	fsrq	343.6	16.3	273 ± 56	0.86
1FLE J2311+3404	4FGL J2311.0+3425	fsrq	348.0	34.1	13.3 ± 4.4	1.82
1FLE J2320-0409	4FGL J2323.5-0317	fsrq	350.0	−4.2	8.6 ± 2.9	1.39
1FLE J2329+0858	4FGL J2327.5+0939	fsrq	352.5	9.0	10.6 ± 3.5	1.84
1FLE J2330-4033	4FGL J2328.3-4036	fsrq	352.5	−40.6	7.7 ± 2.6	…
1FLE J2329-4929	4FGL J2329.3-4955	fsrq	352.4	−49.5	37 ± 11	0.52
1FLE J2345-1611	4FGL J2345.2-1555	fsrq	356.5	−16.2	15.7 ± 5.2	0.62

Notes. The provided uncertainties on the energy flux measurements are 1σ errors. Classifications are obtained from the blazars' associations in the 4FGL-DR2 catalog. All other quantities obtained from the 1FLE catalog.

[a] Redshift in the 1FLE catalog is obtained from the sources' associations in the Fermi-LAT 3LAC catalog. A redshift of "–" indicates no association or no redshift information.

[b] This is the same blazar discussed in Section 1, TXS 0506+056.

ORCID iDs

R. Abbasi https://orcid.org/0000-0001-6141-4205
M. Ackermann https://orcid.org/0000-0001-8952-588X
J. A. Aguilar https://orcid.org/0000-0003-2252-9514
M. Ahlers https://orcid.org/0000-0003-0709-5631
J. M. Alameddine https://orcid.org/0000-0002-9534-9189
A. A. Alves, Jr. https://orcid.org/0000-0003-0073-3231
G. Anton https://orcid.org/0000-0003-2039-4724
C. Argüelles https://orcid.org/0000-0003-4186-4182
Y. Ashida https://orcid.org/0000-0003-4136-2086
A. Balagopal V. https://orcid.org/0000-0001-5367-8876
S. W. Barwick https://orcid.org/0000-0003-2050-6714
V. Basu https://orcid.org/0000-0002-9528-2009
J. J. Beatty https://orcid.org/0000-0003-0481-4952
J. Becker Tjus https://orcid.org/0000-0002-1748-7367
J. Beise https://orcid.org/0000-0002-7448-4189

C. Bellenghi https://orcid.org/0000-0001-8525-7515
S. BenZvi https://orcid.org/0000-0001-5537-4710
E. Bernardini https://orcid.org/0000-0003-3108-1141
D. Z. Besson https://orcid.org/0000-0001-6733-963X
E. Blaufuss https://orcid.org/0000-0001-5450-1757
S. Blot https://orcid.org/0000-0003-1089-3001
J. Y. Book https://orcid.org/0000-0001-6687-5959
S. Böser https://orcid.org/0000-0002-5918-4890
O. Botner https://orcid.org/0000-0001-8588-7306
F. Bradascio https://orcid.org/0000-0002-7750-5256
S. Bron https://orcid.org/0000-0002-6305-3041
M. A. Campana https://orcid.org/0000-0003-4162-5739
C. Chen https://orcid.org/0000-0002-8139-4106
Z. Chen https://orcid.org/0000-0002-2813-7688
D. Chirkin https://orcid.org/0000-0003-4911-1345
B. A. Clark https://orcid.org/0000-0003-4089-2245
A. Coleman https://orcid.org/0000-0003-1510-1712
G. H. Collin https://orcid.org/0000-0003-1032-6496
J. M. Conrad https://orcid.org/0000-0002-6393-0438
P. Coppin https://orcid.org/0000-0001-6869-1280
P. Correa https://orcid.org/0000-0002-1158-6735
D. F. Cowen https://orcid.org/0000-0003-4738-0787
R. Cross https://orcid.org/0000-0003-0081-8024
P. Dave https://orcid.org/0000-0002-3879-5115
C. De Clercq https://orcid.org/0000-0001-5266-7059
J. J. DeLaunay https://orcid.org/0000-0001-5229-1995
D. Delgado López https://orcid.org/0000-0002-4306-8828
H. Dembinski https://orcid.org/0000-0003-3337-3850
A. Desai https://orcid.org/0000-0001-7405-9994
P. Desiati https://orcid.org/0000-0001-9768-1858
K. D. de Vries https://orcid.org/0000-0002-9842-4068
G. de Wasseige https://orcid.org/0000-0002-1010-5100
T. DeYoung https://orcid.org/0000-0003-4873-3783
A. Diaz https://orcid.org/0000-0001-7206-8336
J. C. Díaz-Vélez https://orcid.org/0000-0002-0087-0693
H. Dujmovic https://orcid.org/0000-0003-1891-0718
M. A. DuVernois https://orcid.org/0000-0002-2987-9691
P. Eller https://orcid.org/0000-0001-6354-5209
P. A. Evenson https://orcid.org/0000-0001-7929-810X
K. L. Fan https://orcid.org/0000-0002-8246-4751
A. R. Fazely https://orcid.org/0000-0002-6907-8020
A. Fedynitch https://orcid.org/0000-0003-2837-3477
A. T. Fienberg https://orcid.org/0000-0002-9472-3597
C. Finley https://orcid.org/0000-0003-3350-390X
D. Fox https://orcid.org/0000-0002-3714-672X
A. Franckowiak https://orcid.org/0000-0002-5605-2219
P. Fürst https://orcid.org/0000-0002-7951-8042
T. K. Gaisser https://orcid.org/0000-0003-4717-6620
J. Gallagher https://orcid.org/0000-0001-8608-0408
E. Ganster https://orcid.org/0000-0003-4393-6944
A. Garcia https://orcid.org/0000-0002-8186-2459
S. Garrappa https://orcid.org/0000-0003-2403-4582
A. Ghadimi https://orcid.org/0000-0002-6350-6485
C. Glaser https://orcid.org/0000-0001-5998-2553
T. Glauch https://orcid.org/0000-0003-1804-4055
T. Glüsenkamp https://orcid.org/0000-0002-2268-9297
S. Goswami https://orcid.org/0000-0002-0373-9770
T. Grégoire https://orcid.org/0000-0001-8711-1456
S. Griswold https://orcid.org/0000-0002-7321-7513
P. Gutjahr https://orcid.org/0000-0001-7980-7285
A. Hallgren https://orcid.org/0000-0001-7751-4489
L. Halve https://orcid.org/0000-0003-2237-6714
F. Halzen https://orcid.org/0000-0001-6224-2417
A. Haungs https://orcid.org/0000-0002-9638-7574
K. Helbing https://orcid.org/0000-0003-2072-4172
F. Henningsen https://orcid.org/0000-0002-0680-6588
C. Hill https://orcid.org/0000-0003-0647-9174
T. Huber https://orcid.org/0000-0002-6515-1673
K. Hultqvist https://orcid.org/0000-0003-0602-9472
N. Iovine https://orcid.org/0000-0001-7965-2252
G. S. Japaridze https://orcid.org/0000-0002-7000-5291
M. Jin https://orcid.org/0000-0003-0487-5595
B. J. P. Jones https://orcid.org/0000-0003-3400-8986
D. Kang https://orcid.org/0000-0002-5149-9767
W. Kang https://orcid.org/0000-0003-3980-3778
A. Kappes https://orcid.org/0000-0003-1315-3711
T. Karg https://orcid.org/0000-0003-3251-2126
M. Karl https://orcid.org/0000-0003-2475-8951
A. Karle https://orcid.org/0000-0001-9889-5161
U. Katz https://orcid.org/0000-0002-7063-4418
M. Kauer https://orcid.org/0000-0003-1830-9076
J. L. Kelley https://orcid.org/0000-0002-0846-4542
A. Kheirandish https://orcid.org/0000-0001-7074-0539
S. R. Klein https://orcid.org/0000-0003-2841-6553
A. Kochocki https://orcid.org/0000-0003-3782-0128
R. Koirala https://orcid.org/0000-0002-7735-7169
H. Kolanoski https://orcid.org/0000-0003-0435-2524
L. Köpke https://orcid.org/0000-0001-8530-6348
C. Kopper https://orcid.org/0000-0001-6288-7637
D. J. Koskinen https://orcid.org/0000-0002-0514-5917
P. Koundal https://orcid.org/0000-0002-5917-5230
M. Kovacevich https://orcid.org/0000-0002-5019-5745
M. Kowalski https://orcid.org/0000-0001-8594-8666
E. Kun https://orcid.org/0000-0003-2769-3591
N. Kurahashi https://orcid.org/0000-0003-1047-8094
C. Lagunas Gualda https://orcid.org/0000-0002-9040-7191
M. J. Larson https://orcid.org/0000-0002-6996-1155
F. Lauber https://orcid.org/0000-0001-5648-5930
J. P. Lazar https://orcid.org/0000-0003-0928-5025
J. W. Lee https://orcid.org/0000-0001-5681-4941
K. Leonard https://orcid.org/0000-0002-8795-0601
A. Leszczyńska https://orcid.org/0000-0003-0935-6313
Q. R. Liu https://orcid.org/0000-0003-3379-6423
E. Lohfink https://orcid.org/0000-0003-3248-5682
L. Lu https://orcid.org/0000-0003-3175-7770
F. Lucarelli https://orcid.org/0000-0002-9558-8788
A. Ludwig https://orcid.org/0000-0001-9038-4375
W. Luszczak https://orcid.org/0000-0003-3085-0674
Y. Lyu https://orcid.org/0000-0002-2333-4383
W. Y. Ma https://orcid.org/0000-0003-1251-5493
J. Madsen https://orcid.org/0000-0003-2415-9959
I. C. Mariş https://orcid.org/0000-0002-5771-1124
R. Maruyama https://orcid.org/0000-0003-2794-512X
F. McNally https://orcid.org/0000-0002-0785-2244
K. Meagher https://orcid.org/0000-0003-3967-1533
M. Meier https://orcid.org/0000-0002-9483-9450
S. Meighen-Berger https://orcid.org/0000-0001-6579-2000
T. Montaruli https://orcid.org/0000-0001-5014-2152
R. W. Moore https://orcid.org/0000-0003-4160-4700
M. Moulai https://orcid.org/0000-0001-7909-5812
R. Naab https://orcid.org/0000-0003-2512-466X
R. Nagai https://orcid.org/0000-0001-7503-2777
J. Necker https://orcid.org/0000-0003-0280-7484
H. Niederhausen https://orcid.org/0000-0002-9566-4904

M. U. Nisa https://orcid.org/0000-0002-6859-3944
S. C. Nowicki https://orcid.org/0000-0003-2497-8057
A. Obertacke Pollmann https://orcid.org/0000-0002-2492-043X
B. Oeyen https://orcid.org/0000-0003-2940-3164
E. O'Sullivan https://orcid.org/0000-0003-1882-8802
H. Pandya https://orcid.org/0000-0002-6138-4808
N. Park https://orcid.org/0000-0002-4282-736X
E. N. Paudel https://orcid.org/0000-0001-9276-7994
C. Pérez de los Heros https://orcid.org/0000-0002-2084-5866
J. Peterson https://orcid.org/0000-0002-7985-1443
A. Pizzuto https://orcid.org/0000-0002-8466-8168
M. Plum https://orcid.org/0000-0001-8691-242X
A. Porcelli https://orcid.org/0000-0002-3220-6295
C. Raab https://orcid.org/0000-0001-9921-2668
M. Rameez https://orcid.org/0000-0001-5023-5631
A. Rehman https://orcid.org/0000-0001-7616-5790
E. Resconi https://orcid.org/0000-0003-0705-2770
S. Reusch https://orcid.org/0000-0002-7788-628X
W. Rhode https://orcid.org/0000-0003-2636-5000
B. Riedel https://orcid.org/0000-0002-9524-8943
M. Rongen https://orcid.org/0000-0002-7057-1007
C. Rott https://orcid.org/0000-0002-6958-6033
D. Ryckbosch https://orcid.org/0000-0002-8759-7553
D. Rysewyk Cantu https://orcid.org/0000-0002-3612-6129
I. Safa https://orcid.org/0000-0001-8737-6825
D. Salazar-Gallegos https://orcid.org/0000-0002-9312-9684
A. Sandrock https://orcid.org/0000-0002-6779-1172
M. Santander https://orcid.org/0000-0001-7297-8217
S. Sarkar https://orcid.org/0000-0002-1206-4330
S. Sarkar https://orcid.org/0000-0002-3542-858X
K. Satalecka https://orcid.org/0000-0002-7669-266X
H. Schieler https://orcid.org/0000-0002-2637-4778
S. Schindler https://orcid.org/0000-0001-5507-8890
A. Schneider https://orcid.org/0000-0002-0895-3477
J. Schneider https://orcid.org/0000-0001-7752-5700
F. G. Schröder https://orcid.org/0000-0001-8495-7210
L. Schumacher https://orcid.org/0000-0001-8945-6722
S. Sclafani https://orcid.org/0000-0001-9446-1219
A. Sharma https://orcid.org/0000-0001-5397-6777
M. Silva https://orcid.org/0000-0001-6940-8184
B. Smithers https://orcid.org/0000-0003-1273-985X
J. Soedingrekso https://orcid.org/0000-0003-1011-2797
D. Soldin https://orcid.org/0000-0003-3005-7879
G. M. Spiczak https://orcid.org/0000-0002-0030-0519
C. Spiering https://orcid.org/0000-0001-7372-0074
R. Stein https://orcid.org/0000-0003-2434-0387
J. Stettner https://orcid.org/0000-0003-1042-3675
T. Stezelberger https://orcid.org/0000-0003-2676-9574
T. Stuttard https://orcid.org/0000-0001-7944-279X
G. W. Sullivan https://orcid.org/0000-0002-2585-2352
I. Taboada https://orcid.org/0000-0003-3509-3457
S. Ter-Antonyan https://orcid.org/0000-0002-5788-1369
W. G. Thompson https://orcid.org/0000-0003-2988-7998
K. Tollefson https://orcid.org/0000-0001-9725-1479
S. Toscano https://orcid.org/0000-0002-1860-2240
A. Trettin https://orcid.org/0000-0003-0350-3597
C. F. Tung https://orcid.org/0000-0001-6920-7841
A. Turcati https://orcid.org/0000-0002-8050-7869
M. A. Unland Elorrieta https://orcid.org/0000-0002-6124-3255
N. Valtonen-Mattila https://orcid.org/0000-0002-1830-098X
J. Vandenbroucke https://orcid.org/0000-0002-9867-6548
N. van Eijndhoven https://orcid.org/0000-0001-5558-3328
J. van Santen https://orcid.org/0000-0002-2412-9728
S. Verpoest https://orcid.org/0000-0002-3031-3206
C. Walck https://orcid.org/0000-0002-4188-9219
T. B. Watson https://orcid.org/0000-0002-8631-2253
C. Weaver https://orcid.org/0000-0003-2385-2559
J. Weldert https://orcid.org/0000-0002-3709-2354
C. Wendt https://orcid.org/0000-0001-8076-8877
N. Whitehorn https://orcid.org/0000-0002-3157-0407
C. H. Wiebusch https://orcid.org/0000-0002-6418-3008
M. Wolf https://orcid.org/0000-0001-9991-3923
S. Yoshida https://orcid.org/0000-0003-2480-5105
T. Yuan https://orcid.org/0000-0002-7041-5872
Z. Zhang https://orcid.org/0000-0002-7347-283X

References

Aartsen, M. G., Abbasi, R. U., Abdou, Y., et al. 2013, Sci, 342, 1242856
Aartsen, M. G., Abraham, K., Ackermann, M., et al. 2015, ApJ, 809, 98
Aartsen, M. G., Abraham, K., Ackermann, M., et al. 2016, PhRvD, 93, 022001
Aartsen, M. G., Ackermann, M., Adams, J., et al. 2017a, JInst, 12, P03012
Aartsen, M. G., Abraham, K., Ackermann, M., et al. 2017b, ApJ, 835, 45
Aartsen, M. G., Abraham, K., Ackermann, M., et al. 2017, ApJ, 835, 151
Aartsen, M. G., Ackermann, M., Adams, J., et al. 2018a, Sci, 361, eaat1378
Aartsen, M. G., Ackermann, M., Adams, J., et al. 2018b, Sci, 361, 147
Aartsen, M. G., Ackermann, M., Adams, J., et al. 2020a, PhRvL, 124, 051103
Aartsen, M. G., Ackermann, M., Adams, J., et al. 2020b, ApJ, 898, 117
Aartsen, M. G., Abbasi, R., Ackermann, M., et al. 2021a, Natur, 591, 220
Aartsen, M. G., Abbasi, R., Ackermann, M., et al. 2021, JPhG, 48, 060501
Abbasi, R., Abe, M., Abu-Zayyad, T., et al. 2016, APh, 80, 131
Abbasi, R., Ackermann, M., Adams, J., et al. 2021, arXiv:2101.09836
Abbasi, R., Ackermann, M., Adams, J., et al. 2022, ApJ, 928, 50
Abdollahi, S., Acero, F., Ackermann, M., et al. 2020, ApJS, 247, 33
Abreu, P., Aglietta, M., Albury, J. M., et al. 2021, EPJC, 81, 966
Ackermann, M., Ajello, M., Allafort, A., et al. 2011, ApJ, 743, 171
Ajello, M., Atwood, W. B., Baldini, L., et al. 2017, ApJS, 232, 18
Arámburo-García, A., Bondarenko, K., Boyarsky, A., et al. 2021, PhRvD, 104, 083017
Atwood, W. B., Abdo, A. A., Ackermann, M., et al. 2009, ApJ, 697, 1071
Berezinskii, V. S., & Smirnov, A. I. 1975, Ap&SS, 32, 461
Braun, J., Dumm, J., De Palma, F., et al. 2008, APh, 29, 299
Böttcher, M., Reimer, A., Sweeney, K., & Prakash, A. 2013, ApJ, 768, 54
Cerruti, M., Zech, A., Boisson, C., et al. 2019, MNRAS, 483, L12
De Angelis, A., Tatischeff, V., Grenier, I., et al. 2018, JHEAp, 19, 1
Fleischhack, H. 2021, ICRC (Berlin), 37, 649
Fossati, G., Maraschi, L., Celotti, A., Comastri, A., & Ghisellini, G. 1998, MNRAS, 299, 433
Gao, S., Pohl, M., & Winter, W. 2017, ApJ, 843, 109
Haack, C., & Wiebusch, C. 2017, ICRC (Busan), 35, 1005
Halzen, F., & Zas, E. 1997, ApJ, 488, 669
Huber, M. 2019, ICRC (Madison, WI), 36, 916
Mannheim, K., Biermann, P. L., & Kruells, W. M. 1991, A&A, 251, 723
Mannheim, K., Protheroe, R. J., & Rachen, J. P. 2000, PhRvD, 63, 023003
Murase, K., Guetta, D., & Ahlers, M. 2016, PhRvL, 116, 071101
Ojha, R., Zhang, H., Kadler, M., et al. 2019, BAAS, 51, 431
Principe, G., Malyshev, D., Ballet, J., & Funk, S. 2018, A&A, 618, A22
Urry, C. M., & Padovani, P. 1995, PASP, 107, 803
Zyla, P. A., Barnett, R. M., Beringer, J., et al. 2020, PTEP, 2020, 083C01